

# Trophallaxis among swarm-robots: A biologically inspired strategy for swarm robotics

Thomas Schmickl, and Karl Crailsheim

*Department for Zoology  
Karl-Franzens-Universität Graz  
Universitätsplatz 2, A-8010 Graz, Austria  
[schmickl@nextera.at](mailto:schmickl@nextera.at), <http://zool33.uni-graz.at/schmickl/>*

**Abstract** – This article presents a bio-inspired communication strategy for large-scale robot swarms. The strategy is based on robot-to-robot interactions without any central communication unit. Thus, the emerging swarm regulates itself in a purely self-organized way. The strategy is biologically inspired by the trophallactic behavior performed by social insects. The experiments shown in this article are performed with a simulation environment that was developed to model the properties of a specific type of swarm robot. We investigated the suggested communication strategy in several arena scenarios and studied the properties of some emergent collective decisions made by the robots.

**Index Terms** – swarm robotics, communication, honey bee, trophallaxis

## I. INTRODUCTION

Within a swarm of many small-sized robots, a decentralized strategy of communication is crucial. Usually, the abilities of swarm-robots to communicate are very limited and communication is affected by noise. The study presented here is focused on a swarm of 200 robots. The focal robots communicate by 6 infrared LEDs and photodiodes. Our goal was to develop a method which allows the robots to regulate the swarm behavior autonomously without a central unit of control. The emerging behavior is desired to be self-organized and our aim was to observe a possible example of “swarm intelligence” within the robot swarm.

The project is part of the EU funded I-SWARM project [1] which has the goal to develop a swarm of 1000 very small (I-SWARM robots, approx. 2mm x 2mm) robots, and a swarm of several tens or hundreds of bigger sized robots (JASMINE robots, approx. 3cm x 3cm). The swarm of the JASMINE robots [2] is aimed to test several control strategies for the final I-SWARM robots. Prior to such hardware-tests, we use a tailored simulation platform to develop, tune and test a variety of control strategies.

The control strategy we present here is inspired by the trophallactic behavior of social insects. Trophallaxis is the exchange of fluid food by direct mouth-to-mouth contacts. Trophallaxis is found in insects (honey bees, wasps, bumble bees, ants, and termites) but also in mammals (vampire bats) and birds. The trophallactic behavior of

honeybees is reviewed in detail in [3]. [4, 5] showed, that trophallaxis plays an important role in the regulation of collective foraging decisions in honeybees. Our method is derived from the following example:

An artificial feeder offering sugar solution is installed into a honeybee hive. A honeybee which finds the feeder fills its nectar crop with the offered sugar solution (*addition-rate*). Afterwards it walks towards a honey-storage comb. During its way through the hive, the bee constantly spends energy which is derived from consuming a fraction of the sugar solution load. The higher the metabolic rate of the bee is, the higher this *consumption-rate* will be. If the bee meets another bee on its way, there can be a trophallactic contact. This contact shifts expectedly a fraction of sugar solution of the bee with the higher crop load to the bee with the lower crop load (*transfer-rate*). This way, a gradient of crop load sizes could emerge within a honeybee colony, especially when the sugar-feeder is the only source for crop loads. The shorter the distances between the feeder and a randomly picked bee is, the higher its current crop-load can be expected. Currently, in honeybees, the importance of such a mechanism is unclear; our lab currently researches honeybee trophallactic behavior in a FWF-funded project.

We transferred the scenario described above into the context of a multi-robotic cleaning scenario: An area of dirt, where empty robots shall aggregate, functions like the artificial feeder in the honeybee colony. The crop loads of bees are represented by internal variables (floating-point numbers) in each robots memory. To allow efficient navigation of the robots, we extended the strategy by an additional point: Each robot can query the “nutritional” status of the robots in its local neighborhood and use this information to navigate uphill in the gradient. When the swarm has to navigate between two targets, we establish two distinct gradients in parallel by allowing the robots to have two internal variables and by transferring the values in parallel by two distinct communication channels.

## II. METHODS

We used a down-scaled version of LaRoSim (= Large robot swarm simulator) V0.26a to perform the simulation experiments described in this article. The full-scale LaRoSim simulator treats 1000 small robots (unpublished) simultaneously in the arena, while the down-scaled version is intended to treat 100-200 of the bigger sized robots. The simulation environment was implemented modularly, so

---

\* This work is supported by the EU IST-FET-open project (IP) ‘I-Swarm’, no. 507006 and by the FWF funded project P 15961-B06.

that we now can investigate a variety of bio-inspired control-strategies for robot swarms in this environment, thus allowing comparison of the gained results. The “trophallaxis-derived strategy” is the first to be published; other strategies will be published separately.

For testing the suggested trophallaxis-derived strategy, we designed a cleaning scenario containing one area of dirt and one area designated as “dump”. The goal for the robots was to pick up the dirt, to transfer the dirt items to the dump and to drop the dirt items there. In the first tested simulation scenario, the robots can directly move from the dirt area to the dump area. In a second simulation experiment, the journey of a loaded robot was made more difficult by a wall which was placed across the arena and which had to be passed by the robots through one of two gates. Basically the ways from dirt to dump through the two gates were of equal length. In additional variations of the 2<sup>nd</sup> scenario, the locations of the gates in the wall were shifted, so that the two possible paths vary in their length.

Our simulated robots move by two wheels that can be driven separately, allowing curves and on-the-place rotations. The communicating abilities of the robots are simulated accordingly to the design of the real JASMINE robots: 6 infrared LEDs allow collision avoidance and wall avoidance. Robot-to-robot communication is provided by 6 photodiodes in addition to the LEDs. The robots actively avoid each other by a potential-field based method. Loaded robots have a higher repulsive potential than empty ones.

Each robot carries an additional Boolean (on/off) signal that communicates its loading state. Fig. 1 displays a scheme of the morphology of simulated robots. The simulator assumes a blind spot of approx. 30 degrees in between each neighboring pair of emitted LED light cones, but no blind spot for the photodiodes. The processes involved in the communication are depicted in Fig. 2. The following four equations describe the mathematics of the trophallaxis-derived control strategy:  $n$  is an index that allows distinction of the two used internal variables ( $v_1$  and  $v_2$ ).  $i$  is an index that specifies the robot that currently executes the equations. Equation (1) shows that the value of  $v_{n,i}$  is affected by three terms per time step:

- 1.)  $c_{n,i}(t)$ , is a steady reduction of the value of  $v_n$  by the constant consumption-rate  $cr_n$  (2).
- 2.) The communicated value of the trophallactic transfer of variable  $v_n$  between robot  $i$  and robot  $j$  is denoted as  $t_{n,i,j}(t)$ . This value is calculated by using a given constant transfer-rate  $tr_n$  (3).  $v_{n,j}$  is the value of the internal variable  $v_n$  of the nearest neighbor. If the trophallactic transfer shall be performed with more than one neighbor, then (3) has to be performed with all neighbors one after another, and the shared amount of  $v_n$  is decreased proportionally.
- 3.) The increment of the value of  $v_{n,i}$  triggered by an encounter of a piece of dirt (if  $n=1$ ) or by an encounter of the dump area (if  $n=2$ ). In both cases, a constant addition-rate  $ar_n$  is added to  $v_{n,i}$  (4).

Equations (1), (2), (3) and (4) lead to a gradient which emerges from the point where  $a_{n,i}$  is triggered. In our

simulations, we wanted to have two gradients, one pointing towards the dirt (to be followed by empty robots) and one pointing towards the dump (to be followed by loaded robots).

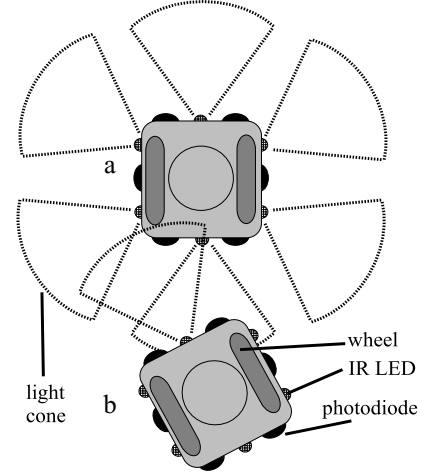


Fig. 1 Morphology of the robots in the used simulation environment with special emphasis on the communication system (infrared LEDs, photodiodes) and on the movement systems. In the picture, the two robots can establish a bidirectional communication. In the picture, all 6 light cones of robot “a” are drawn, only the one light cone that is involved into a communication channel is drawn for robot “b”.

$$v_{n,i}(t+1) = v_{n,i}(t) - c_{n,i}(t) - t_{n,i,j}(t) + a_{n,i}(t) \quad (1)$$

$$c_{n,i}(t) = v_{n,i}(t) \cdot cr_n \quad (2)$$

$$t_{n,i,j}(t) = (v_{n,i}(t) - v_{n,j}(t)) \cdot tr_n \quad (3)$$

$$a_{n,i}(t) = \begin{cases} ar_n & \dots \text{if } ((n=1) \wedge (\text{robot}_i \text{ is on dirt})) \vee \\ & ((n=2) \wedge (\text{robot}_i \text{ is on dump})) \\ 0 & \dots \text{else} \end{cases} \quad (4)$$

First preliminary results showed a general problem that arises if all robots walk uphill too strictly in the gradients: Most robots aggregate near the dirt and near the dump and the other areas of the arena are almost empty. If this happens, the “bridging” of information between dirt and dump gets lost. To prevent this undesirable status of the robot swarm, we prevented 15% of the robots from moving uphill in the gradients (*percentage-pure-communicators*). These robots perform a random walk with obstacle avoidance and perform all communicational processes described in equations (1) to (4). In addition to that, the empty robots followed the gradient established by  $v_1$  only in 33% of all time steps (*weight-strategy-to-dirt*), while the loaded robots followed the other gradient, established by  $v_2$  in every time step (*weight-strategy-to-dump*).

In total we performed two sets of experiments: In scenario one, the robots were able to pass directly from the dirt area in the lower left corner to the dump area in the upper right corner (Fig. 3). In a second experiment, the way was blocked by a diagonal wall that has to be passed by two small gates. The resulting two ways from the dirt to the dump were of equal length (Fig.4).

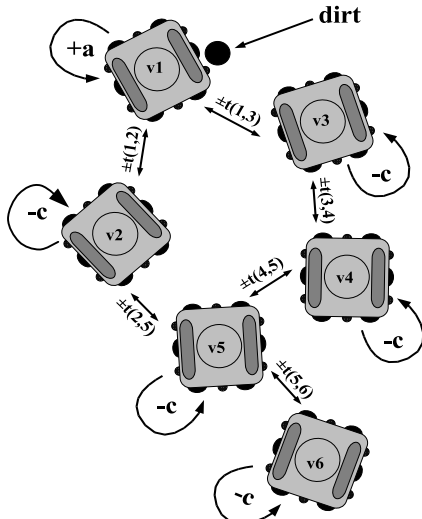


Fig. 2 This scheme shows the basic principles of the “trophallaxis derived control strategy”. Robot 1 finds a piece of dirt and increases its internal variable  $v$  by the given addition rate  $(+a)$ . All robots constantly decrease their internal variable  $v$  by the given consumption rate  $(-c)$ . The variable  $v$  is constrained to be above zero. All robots that are near enough to establish a robot-to-robot communication link communicate their current values of  $v$  and transfer a fraction of the encountered difference from the robot with the higher value of  $v$  to the robot with the lower value of  $v$   $(\pm t)$

To allow the simulation environment to make plausible predictions of the real robot swarm’s behavior, we applied several sources of noise on the communication and on the sensory inputs. This noise was defined as a probability of a total break of communication, as a uniform random noise on measurements of distances, on measurements of angles and on the communicated values during the “trophallactic transfers”. In our simulation environment, the floor is constructed in discrete way, by setting colors and other properties of “patches”. In contrast to that, the robots move in continuous routes over that floor. One patch corresponds to 3cm x 3cm, what corresponds approximately to the size of the JASMINE robots. In our simulations presented here, robot speed was restricted to 0.5 patches per time step, what corresponds to a maximum robot speed of 1.5cm/second. The robots can sense the dump and the dirt only when they are already located on it. Initially, we distributed the robots (all empty) randomly on the arena; each robot was facing into a randomized direction.

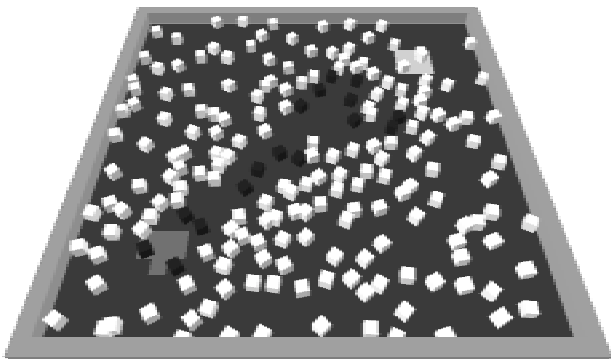


Fig. 3 A screenshot of the simulated robot swarm in the first investigated cleaning scenario: The swarm consisted of 200 robots. The brighter patches on the floor in the left lower corner indicate dirt areas, the brighter patches in the right upper corner indicate the dump areas. Empty robots are colored in white, loaded robots are colored in black.

In all our scenarios, the Euclidean distance between dirt and dump was 22.6 patches. In total, 36 pieces of dirt were placed initially in the arena; the simulations were stopped after the last piece of dirt was correctly transferred to the dump. We had an additional “stop-condition”, which breaks the simulation runs after 1000 time steps (corresponds to 16.66 min in reality), but this stop condition was never triggered in a simulation run. In both simulation scenarios, we used the same parameter settings for the robot swarm (table 1).

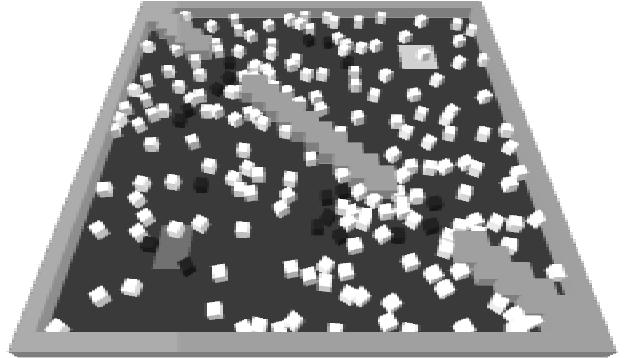


Fig. 4 A screenshot of the simulated robot swarm in the second investigated cleaning scenario: The swarm consisted of 200 robots. The brighter patches on the floor in the left lower corner indicate dirt areas, the brighter patches in the right upper corner indicate the dump areas. Empty robots are colored in white, loaded robots are colored in black. A diagonal wall has to be passed through one of two gates. In the parameter setting shown in this figure, both paths from the dirt to the dump are of equal distance. In other simulation settings, these two paths differ concerning their lengths.

TABLE I  
PARAMETERS USED IN SIMULATIONS. COLUMN ‘S’ INDICATES THE SOURCE OF PARAMETER VALUES: ‘\*’: DERIVED FROM HARDWARE SPECIFICATIONS; ‘+’: VALUES DERIVED FROM PRELIMINARY EXPERIMENTS.

No.	Parameter	S	Value
1	sensory-range	+	5 robot diameters
2	$ar_1$	+	150
3	$ar_2$	+	100
4	$cr_1 = cr_2$	+	0.003
5	$tr_1 = tr_2$	+	0.1
6	collision-avoidance-loaded	+	0.25 * sensory-range
7	collision-avoidance-empty	+	0.75 * sensory-range
8	avoidance-loaded-by-empty	+	0.5 * sensory-range
9	P(error-communication-break)	*	10%
10	error-angle-measurement	*	15 degrees
11	error-distance-measurement	*	10%
12	general-communication-error	*	10%
13	LED-cone-angle	*	30°
14	weight-strategy-to-dirt	+	33%
15	weight-strategy-to-dump	+	100%
16	percentage-pure-communicators	+	15%

### III. RESULTS

#### A. Emerging paths of loaded robots

In the first scenario (Fig. 3), all robots successfully deposited the dirt in the dump. There was no blocking diagonal wall and the robots approached the dump on a direct path as soon as they left the dirt area, due to the information they got via the trophallaxis-derived strategy. This behavior was impressive, because although the dump was far away (24.6 patches), they were already informed

about the optimal direction to leave the dirt area via our trophallaxis-derived communication strategy. To visualize the path the robots choose, we stored the location of each loaded robot in every time step in a matrix and created a map of “cumulative density of robots”. This map (Fig. 5) clearly shows that almost all robots approached the dump on a directed way.

Path of loaded robots in scenario 1 (no wall)

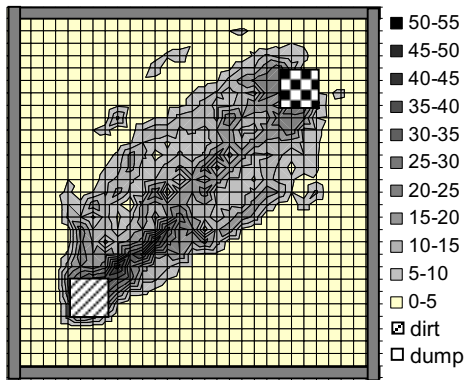


Fig. 5 Cumulative density of all loaded robots throughout a simulation run in scenario 1: A clear direct path emerged; the loaded robots approached the dump directly. The shortest direct way from the dirt to the dump had a length of 24.6 patches. The values on the right indicate how many time steps a patch was occupied by a loaded robot.

In scenario 2, all loaded robots successfully passed through the gates in the diagonal wall and approached the dump (Fig. 6). In an additional simulation run, we simulated an arena containing 2 paths with different length by shifting the left upper gate further away from the center of the wall and by shifting the right lower gate nearer to the center of the wall. The longer path was of length of 38.1 patches, while the shorter path was of length of 26.8 patches. Fig. 7 clearly shows that a majority of the loaded robots took the shorter way through the right lower gate in the diagonal wall.

### B. Emerging distribution of empty robots

As Fig. 8 shows, the empty robots were distributed more evenly than the loaded robots. Nevertheless there was a clear aggregation of empty robots around the area of the dirt (lower left corner). The observed distribution was caused by several factors:

- 1.) The empty robots had a significantly lower *weight-strategy-to-dirt*, what lead to a higher proportion of random movements.
- 2.) In our simulation, 15% of all robots didn't move uphill in the gradient due to the setting of *percentage-pure-communicators*.
- 3.) There were always much more empty robots than loaded ones, so the collision avoidance behavior drove many empty robots into vast areas. This is due to the higher repulsive potential fields emitted by loaded robots in the used collision avoidance algorithm.

The higher number of empty robots is also responsible for the higher cumulative robot densities depicted in Fig. 8 compared to the cumulative densities depicted in Figs. 5-7.

Paths of loaded robots in scenario 2 (symmetric gates)

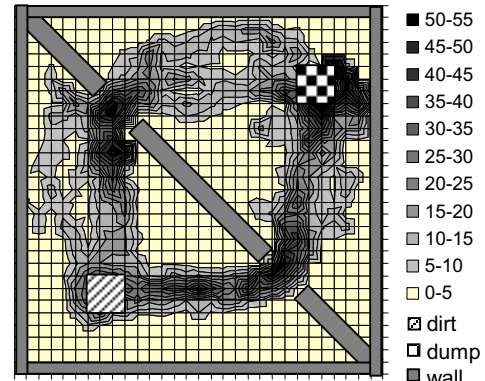


Fig. 6 Cumulative density of all loaded robots throughout a simulation run in scenario 2: Two clear paths emerged, the loaded robots approached both goals at equal rate and went almost directly from dirt to one gate and from the chosen gate to the dump. The two possible paths had both an equal length of 30.3 patches. The values on the right indicate how many time steps a patch was occupied by a loaded robot.

Paths of loaded robots in scenario 2 (asymmetric gates)

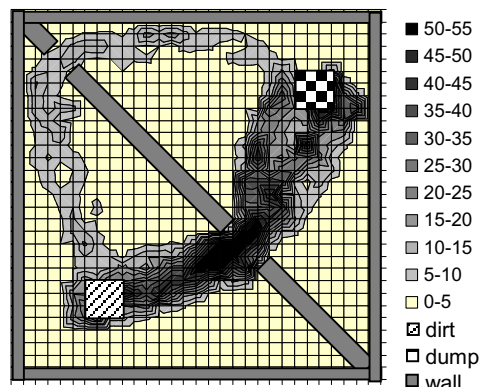


Fig. 7 Cumulative density of all loaded robots throughout a simulation run in scenario 2, with asymmetric placement of the two gates: A strong path emerges through the gate that allows a shorter pathway for the loaded robots (26.8 patches). Only a small fraction of the robots went through the other gate, which allowed only a longer path from dirt to dump (38.1 patches). The values on the right indicate how many time steps a patch was occupied by a loaded robot.

Densities of empty robots in scenario 1 (no wall)

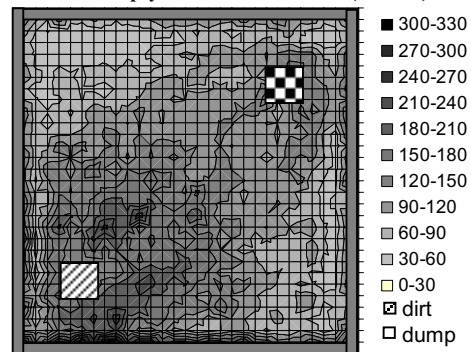


Fig. 8 Cumulative density of all empty robots throughout a simulation run in scenario 1: The robots tended to aggregate loosely around the pieces of dirt, but this aggregation was much weaker than the aggregation of loaded robots on their way from the dirt to the dump in the figures 5, 6, and 7. The values on the right indicate how many time steps a patch was occupied by an empty robot.

### C. Efficiency of transport

We compared the time period it took the robots to deposit all pieces of dirt in all three cases depicted in Fig. 5 – Fig. 7. Fig. 9 shows, that there are small but significant differences in these time periods: Without a wall, it took the robots on average  $420.3 \pm 77.5$  time steps (mean  $\pm$  standard deviation). With the symmetric setting, i.e. with the diagonal wall having symmetrically positioned gates, it took the robots on average  $434.2 \pm 31.2$  time steps to complete the task. With the asymmetric wall setting, it took the robots on average  $508.9 \pm 139.9$  time steps to complete the given task. Both setups, without the diagonal wall ( $N_1=N_2=12$ ,  $z=-3.11$ ,  $P<0.01$ , two-tailed Mann-Whitney U-test) and with diagonal wall with symmetric gates ( $N_1=N_2=12$ ,  $z=-2.25$ ,  $P<0.05$ , two-tailed Mann-Whitney U-test) were proven to allow the robots a faster finishing of the task compared to the asymmetric setting of gates. As Fig. 9 shows, the setting without wall allowed also a faster finishing of the task compared to the wall setup with symmetric gates ( $N_1=N_2=12$ ,  $z=-2.19$ ,  $P<0.05$ , two-tailed Mann-Whitney U-test).

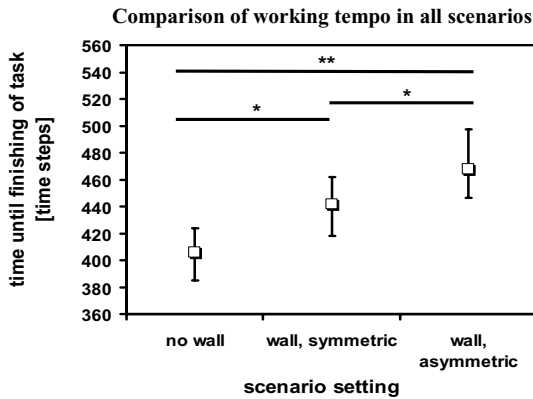


Fig. 9 Time it took the robots to complete their task to deposit all 36 pieces of dirt in the dump. Boxes: median values. Whiskers: 1st quartile to 3rd quartile.  $N = 12$  per setting. Significance: two-tailed Mann-Whitney-U-test, \*:  $P<0.05$ , \*\*:  $P<0.01$ .

### D. Emergent path decisions made by the robot swarm

Figure 9 shows the impact of the gate positions on the robot swarms overall performance. After finding this result, we tested the robot swarm systematically with different levels of asymmetry concerning the position of the gates. An *asymmetry-index* of 0 corresponds to the arena setup depicted in Fig. 4 and Fig. 6. An *asymmetry-index* of 1 corresponds to a more extreme version of the arena setup depicted in Fig. 7, having the left gate shifted to the very end of the diagonal wall. All *asymmetry-indices* between 0 and 1 scale the position of the left gate on the diagonal wall in a linear manner. In all of these setups, the right gate provides the shortest path from the dirt area to the dump area. As Fig. 10 shows, the higher the setups get asymmetric, thus the bigger the difference between long and short path gets, the sharper the swarm makes the collective decision to favor the shorter (right) path.

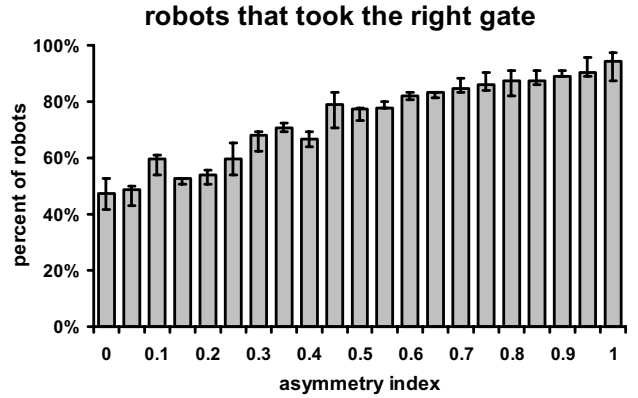


Fig. 10 Collective decision making of the robot swarm in the two-path setups: The higher the difference of length between the short path and the long path gets, the higher was the fraction of robots that took the shorter path. Bars show median values, the whiskers indicate the span between the 1st and the 3rd quartile.  $N=6$  per setting.

## IV. DISCUSSION

In general, our simulation experiments successfully tested and evaluated a new control strategy of a large-scale robot swarm. The used simulator produced sound and stable results. In all cases, the robots successfully found the dirt, and transported it in a directed way (no random walk) to the dump. The suggested cleaning scenario is very similar to the collective food foraging performed by social insects, where food items have to be discovered in the environment and have to be carried to the nest afterwards. On the first sight, the emerging paths look similar to the pheromone trails found in ants and termites. But there are several significant differences found on both, on the proximate level and on the level of ultimate results:

A pheromone is a substance that is released into the environment in very small portions. In case of ant trails, these pheromones are dropped on the ground, stay there and decay after some time. In our robot swarm, nothing (except dirt) is dropped on the arena floor, the whole system works within the emerging communication network and within the memory of the robots. There are important differences of our suggested control strategy to an ant-like pheromone trail: The values of the internal variables  $v_{n,i}$  are not stable concerning their position in the arena. As the robots move through the arena, they take these memory places with them. Local changes of the values of  $v_{n,i}$  lead to different movement patterns of the robot. This affects the local robot densities and this again affects the transfer of values of  $v_{n,i}$ . These differences lead to significantly different results when we compared the ultimate results of our robot swarm to experiments performed with ants. In a setup with two possible paths of the same length, ants chose always one of the 2 ways (see [6] for details, the nonlinearity of ant foraging decisions is described in [7]). In contrast to that, our robot swarm equally distributes on both paths. This is a desired solution, because it helps to prevent traffic jams in a crowded arena.

In contrast to ants, which can be trapped in prior foraging decisions (c.f. from [8]), honeybees are able to revert prior decisions [9, 10, 11]. First preliminary

experiments suggest, that also our robot swarm can “re-decide” in fluctuating environments (data not shown). Some other approaches have been developed to allow swarm behavior in similar ways, but these approaches show significant differences to the algorithm suggested by us: [12] used a system of communicated hop-counts to generate a gradient field in the arena. Other studies [13] used a geometric-based algorithm to spread autonomous robots in an arena. The evolution of collective aggregation behavior of a robot swarm was studied by [14]. The ability to approach a given target autonomously by phototaxis and by optomotor behavior was investigated by [15].

The given task is a hard problem for robots that have no vision (no camera on board). Although they can sense obstacles and other robots by their horizontal LEDs, they can detect dirt items and the dump area only when they are already directly located on them. So the sensory range for the focal places (dirt and dump) is limited to a robot’s own size. This very poor sensory capability is compensated by forcing the swarm of unloaded robots to spread through the arena and to perform a systematic search. The suggested communication strategy, which is derived from the trophallaxis behavior found in social insects, allows these random explorers to aggregate in interesting areas as soon as the first dirt items are found accidentally by individual robots. This collective strategy is purely based on local robot-to-robot communication, so our suggested robot swarm fulfills all demands to be called “self-organized” and to show “swarm intelligence”. The loaded robots are informed about the location of the dump by the empty robots via the same communication system and directly approach the dump area (Fig. 5). The emerging transport system is “smart” enough to find passages through walls (Figs. 6, 7) and to select the shortest possible path in cases where there is a significant difference between short and long pathways (Fig. 10). The described system is composed of the following components:

- 1.) The *addition-rate* (4) together with the gradient-following behavior provides a positive feedback loop leading to aggregation on a desired target.
- 2.) The *transfer-rate* (3) leads to a spread of the information and to a linkage of the individuals’ memory places. This way the robots create a shared map of their environment.
- 3.) The *consumption-rate* (2) provides a constant negative feedback loop, which is very important to let outdated information vanish from the system. Without this important negative feedback loop, errors (e.g., due to communication noise) could sum up and let the whole swarm behavior “go mad”.

To prevent traffic jams and to prevent breaks in the communication chains, we forced the empty robots to keep a certain amount of randomness in their movement behavior (Fig. 8). This seems inefficient on the first sight, but it ensures that the whole arena is consequently explored for dirt throughout the experimental period. So far, the robots in our simulation are assumed to be powered by solar-cells ad libitum. The robots populate the arena in high numbers, so we assumed crowding issues to be more

important than energetic efficiency of the swarm. In future simulation experiments we will confront the robot swarm with fluctuating environments by randomly adding new dirt patches into the arena, in these setups the random movements of the empty robots will pay back. If one wants the empty robots to aggregate as sharply on the dirt as the loaded robots head towards the dump, only one parameter (*weight-strategy-to-dirt*) has to be adjusted in our suggested algorithm. In these circumstances, it is crucial to prevent a certain fraction of the robots from aggregation (*percentage-pure-communicators*) to ensure a consistent chain of robot-to-robot communication.

The next steps in development will be an investigation of the trophallaxis-derived strategy in fluctuating environments, the optimization of the parameters shown in table 1 by “Evolutionary Computation” algorithms, and the evaluation of other bio-inspired control strategies in the same cleaning scenario.

## REFERENCES

- [1] J. Seyfried et al., “The I-SWARM Project: Intelligent Small World Autonomous Robots for Micro-Manipulation,” in “Swarm Robotics,” SAB 2004, LNCS 3342, E. Sahin and W.M. Spears, Eds. Springer Verlag, 2005, pp.70-83, 2005.
- [2] [https://ipvszope.informatik.uni-stuttgart.de/ipvs/abteilungen/bv/forschung/projekte/Collective-robotics/Micro-robot\\_Jasmine/Description\\_Jasmine/en](https://ipvszope.informatik.uni-stuttgart.de/ipvs/abteilungen/bv/forschung/projekte/Collective-robotics/Micro-robot_Jasmine/Description_Jasmine/en).
- [3] K. Crailsheim, “The Flow of Jelly within a Honeybee Colony,” *Journal of Comparative Physiology B*, vol. 162, pp. 681-689, 1992.
- [4] S. Camazine, “The Regulation of Pollen Foraging by Honey Bees: How Foragers Assess the Colony’s Need for Pollen,” *Behavioral Ecology and Sociobiology*, vol. 32, pp. 265-273, 1993.
- [5] S. Camazine et al., “Protein Trophallaxis and the Regulation of Pollen Foraging by Honeybees (*Apis mellifera* L.),” *Apidologie*, vol. 29, pp. 113-126, 1998.
- [6] E. Bonabeau, M. Dorigo, and G. Theraulaz, “Swarm Intelligence: From Natural to Artificial Systems,” Santa Fe Institute, Studies in the Sciences of Complexity, 1999.
- [7] D.J.T. Sumpter and M. Beekman, “From Nonlinearity to Optimality: Pheromone Trail Foraging by Ants,” *Animal Behaviour*, vol. 66, pp. 273-280, 2003.
- [8] D.J.T. Sumpter and S.C. Pratt, “A Modelling Framework for Understanding Social Insect Foraging,” *Behavioural Ecology and Sociobiology*, vol. 53, pp. 131-144, 2003.
- [9] T.D. Seeley, S. Camazine, J. Sneyd, “Collective Decision-making in Honey Bees: How Colonies Choose Among Nectar Sources,” *Behavioural Ecology and Sociobiology*, vol. 28, pp. 277-290, 1991.
- [10] T. Schmickl, K. Crailsheim, “Costs of Environmental Fluctuations and Benefits of Dynamic Decentralized Foraging Decisions in Honeybees,” *Adaptive Behavior*, vol. 12, pp.263-277, 2004.
- [11] T. Schmickl, R. Thenius, and K. Crailsheim, “Simulating Swarm Intelligence in Honey Bees: Foraging in Differently Fluctuating Environments,” GECCO’05, Washington, DC, USA, pp. 274-274, June 25-29, 2005.
- [12] D. Payton, R. Estkowski, and M. Howard, “Pheromone Robotics and the Logic of Virtual Pheromones,” in “Swarm Robotics,” SAB 2004, LNCS 3342, E. Sahin and W.M. Spears, Eds. Springer Verlag, 2005, pp.45-57, 2005.
- [13] J. McLurkin and J. Smith, “Distributed Algorithms for Dispersion in Indoor Environments using a Swarm of Autonomous Mobile Robots,” Distributed Autonomous Robotic Systems Conference, June 23, 2004.
- [14] V. Trianni, R. Groß, T.H. Labella, E. Sahin, and M. Dorigo, “Evolving Aggregation Behaviors in a Swarm of Robots,” in ECAL 2003, LNAI 2801, W. Banzhaf et al., Eds. Springer Verlag, 2003, pp. 865-874.
- [15] B. Webb and R. Reeve, “Reafferent or Redundant: Integration of Phototaxis and Optomotor Behavior in Crickets and Robots,” *Adaptive Behaviour*, vol. 11, no. 3, pp. 137-158, 2003.